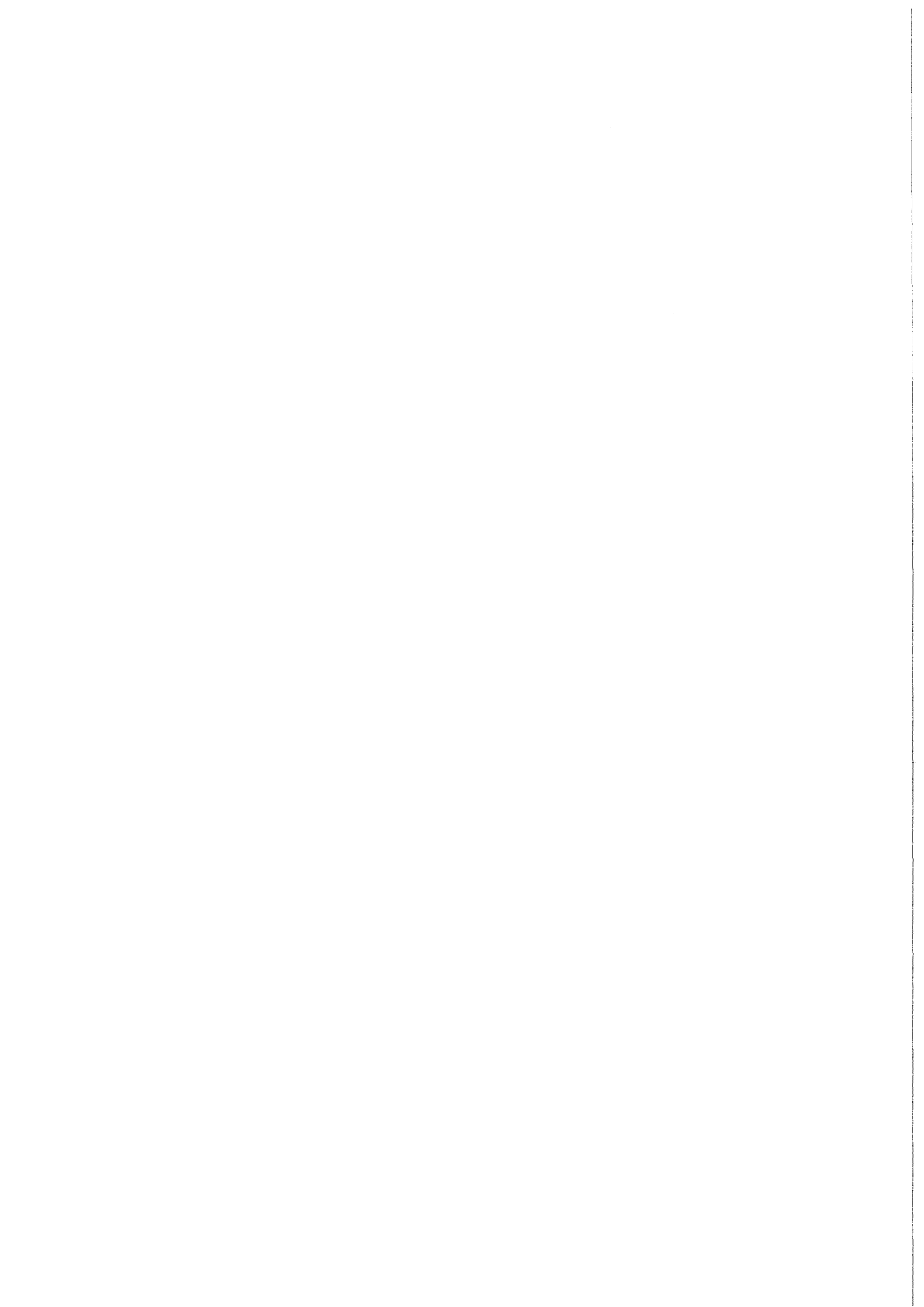


KfK 3536  
Mai 1983

# **Non-Additive Forces in Many-Particle Systems: A Molecular-Dynamics Study for Krypton**

**W. Schommers**  
Institut für Angewandte Kernphysik

**Kernforschungszentrum Karlsruhe**



KERNFORSCHUNGSZENTRUM KARLSRUHE

Institut für Angewandte Kernphysik

KfK 3536

Non-Additive Forces in Many-Particle Systems:  
A Molecular-Dynamics Study for Krypton

W. Schommers

Kernforschungszentrum Karlsruhe GmbH, Karlsruhe

Als Manuskript vervielfältigt  
Für diesen Bericht behalten wir uns alle Rechte vor

Kernforschungszentrum Karlsruhe GmbH  
ISSN 0303-4003

## ABSTRACT

Molecular-dynamics calculations on krypton gas at 297 K have been performed taking into account three-body interactions. The purpose of this paper is to show (i) that the experimental structure data can be well described if we use the Axilrod-Teller form for the three-body potential and (ii) that the three-body potential contribution to dynamic correlations is about one order of magnitude larger than to static correlations. The experimental determination of the dynamic correlation functions can be done with sufficient accuracy by neutron scattering experiments and we expect that the ratio of error to effect for these functions is distinctly smaller than in the case of the structure data. The asymptotic time behaviour of the velocity autocorrelation function has also been investigated. It turned out that the long-time tail is strongly influenced by three-body forces. The famous  $t^{-3/2}$  law has been observed in the calculation with the presence of three-body forces.

## Nichtadditive Kräfte in Vielteilchensystemen: Eine molekular-dynamische Untersuchung für Krypton

### ZUSAMMENFASSUNG

Es wurden molekular-dynamische Rechnungen für gasförmiges Krypton bei einer Temperatur von 297 K unter Berücksichtigung von Dreikörperkräften durchgeführt. Dabei zeigte sich, daß experimentelle Strukturdaten dann gut beschrieben werden, wenn für die Dreikörperwechselwirkung das Axilrod-Teller Potential eingesetzt wird. Außerdem stellte sich heraus, daß dynamische Korrelationsfunktionen um eine Größenordnung auf Dreikörperkräfte empfindlicher sind als statische Korrelationsfunktionen. Dynamische Korrelationsfunktionen für Krypton könnten mit hinreichender Genauigkeit mit Hilfe von Neutronenstreuexperimenten durchgeführt werden; wir erwarten, daß der Quotient aus Meßfehlern zu Effekt für solche Größen deutlich kleiner ist als für

statische Größen. Es wurde außerdem das asymptotische Verhalten der Geschwindigkeits-Selbstkorrelationsfunktion untersucht. Es stellte sich heraus, daß diese Funktion für große Zeiten stark von Dreikörperkräften beeinflusst wird. Das bekannte  $t^{-3/2}$ -Gesetz konnte nur bei Anwesenheit von Dreikörperkräften bestätigt werden.

CONTENTS

Page

Abstract, Kurzfassung

I.	Introduction .....	1
II.	Model .....	1
III.	Structure .....	3
IV.	Dynamic Correlations .....	6
	IV.1 Density Fluctuations .....	6
	IV.2 Mean-Square Displacement .....	11
V.	Asymptotic Time Behaviour of the Velocity	
	Autocorrelation Function .....	13
	V.1 General Remarks .....	13
	V.2 Estimation of the Time-Region .....	14
	V.3 Results and Discussion .....	16
VI.	Summary .....	31
	References .....	32

## I. Introduction

It is well known that three-body interactions cannot be neglected in the correlation functions of noble gases. This has been discussed, for example, in Ref. 1 for liquid argon, and more recently, for krypton gas by Egelstaff and Teitsma<sup>2,3</sup>. Egelstaff and Teitsma performed careful diffraction experiments and analyzed their structure data in terms of the pair potential of Barker et al.<sup>4</sup>; they believe that the differences between the experimental data and the calculated values are due to three-body interactions. In this paper we want to study krypton gas by molecular dynamics (MD). The advantage of this method compared to the methods used in the analysis of Refs. 2 and 3 is that we do not have to restrict our study to static properties and we are also able to investigate dynamic correlations. The purpose of this paper is to show (i) that the experimental structure data given in Refs. 2 and 3 can be well described if we use, for the three-body potential, the Axilrod-Teller form<sup>5</sup>, and (ii) that the three-body contribution to dynamic properties is about one order of magnitude larger than to static correlations which are discussed in Refs. 2 and 3. It should be emphasized that the MD method allows one to study correlation functions without recourse to approximate theories such as the density expansion used in Refs. 2 and 3.

## II. Model

The Hamiltonian used in the calculation is given by

$$H = \sum_{i=1}^N \frac{p_i^2}{2m} + \sum_{i < j=1}^N v_2(i,j) + \lambda \sum_{i < j < l=1}^N v_3(i,j,l), \quad (1)$$

$\lambda$  being an on-off parameter with values 0 and 1. For the pair interaction  $v_2$  we have chosen the potential proposed by Barker et al.<sup>4</sup>; the same potential was used by Egelstaff and Teitsma<sup>2</sup> in their analysis. For the three-body interaction  $v_3$  we have chosen the Axilrod-Teller form<sup>5</sup>

$$v_3(i,j,l) = v \frac{1+3\cos\theta_1\cos\theta_2\cos\theta_3}{r_{ij}^3 r_{il}^3 r_{jl}^3} \quad (2)$$

$r_{ij}$ ,  $r_{il}$ ,  $r_{jl}$  and  $\theta_1$ ,  $\theta_2$ ,  $\theta_3$  are the sides and angles of the triangle formed by the particles  $i, j, l$ .  $v_3(i, j, l)$  can be repulsive and attractive, which depends upon the shape of the triangle formed by the three atoms  $i, j$ , and  $l$ . The parameter  $v$  was chosen to be  $220.4 \times 10^{-84} \text{ cm}^9 \text{ erg}$  (see Ref. 6). In the final analysis, MD results for krypton gas themselves serve as justification for the validity of the chosen potential functions. It should be mentioned that the Axilrod-Teller potential has been used with success in the analysis of argon data<sup>7</sup>.

MD calculations have been performed for the densities  $n = 2.884 \times 10^{27} \text{ atoms/m}^3$  and  $n = 6.19 \times 10^{27} \text{ atoms/m}^3$ . For the MD model,  $N = 128$  krypton atoms were arranged in arbitrary positions in a cubical box of length  $L = 32.42 \text{ \AA}$  ( $L = 27.64 \text{ \AA}$ ), thus providing a density of  $n = 2.884 \times 10^{27} \text{ atoms/m}^3$  ( $n = 6.19 \times 10^{27} \text{ atoms/m}^3$ ). The initial distribution of the velocities was chosen according to Maxwell's distribution. To avoid surface effects, periodical boundary conditions were imposed on the system. For this model the classical Hamilton equations were solved by iteration [time step:  $1.7 \times 10^{-14} \text{ sec}$  ( $1.0 \times 10^{-14} \text{ sec}$ )]. The relative error in the information (positions and velocities) obtained from the iteration process is less than  $10^{-6}$ . We varied the particle number  $N$  and found that  $N$  does not produce any effect in the correlation functions if  $N \geq 128$ : The differences in the results for  $N = 250$  and  $N = 128$  are one order of magnitude smaller than the statistical error. The cut-off radius  $r_c$  for the potentials was chosen to be  $16 \text{ \AA}$  ( $13.5 \text{ \AA}$ ); we found that cut-off effects are ruled out if  $r_c > 14 \text{ \AA}$  ( $11 \text{ \AA}$ ). No further numerical uncertainties appear in a MD calculation except the statistical error in the correlation functions. More details concerning the behavior of MD models are discussed in Refs. 8 and 9.

Using Eq. (1) for the Hamiltonian, two MD calculations for each density have been performed. One with ( $\lambda=1$ ) and another

without ( $\lambda=0$ ) three-body interactions. All calculations were made for  $T = 297$  K according to the diffraction experiments (see Refs. 2 and 3). In the case of  $\lambda=1$  the computer time requirements are very large; using the IBM 3033, the CPU time was approximately five hours.

### III. Structure

To test the model, we have computed the structure factor

$$S(k) = \frac{1}{N} \langle \sum_{i,j} \exp[i\vec{k} \cdot (\vec{r}_i - \vec{r}_j)] \rangle, \quad (3)$$

where  $\vec{r}_i$  is the position vector of particle  $i$  and  $\vec{k}$  the wave vector. Figure 1 shows the MD results for  $S(k)$  obtained from calculations with  $\lambda=0$  and  $\lambda=1$ . The calculations have been performed with high accuracy: The statistical error<sup>10,11</sup> is smaller than 1% for all  $k$  values in Fig. 1; the experimental errors<sup>3</sup> are also smaller than 1%. It can be seen from Fig. 1 that the effects due to the three-body forces are relatively small, and the general agreement with the experimental data is also satisfactory for  $\lambda=0$ . However, there are systematic deviations (which are greater than the errors) from the experimentally observed structure data for the calculations without the presence of the three-body interactions. As can be seen from Fig. 1 these deviations can be described successfully by means of the Axilrod-Teller potential. In contrast to Monte Carlo results<sup>2</sup> we did not find that the principal peak height of the pair correlation function is suppressed by the Axilrod-Teller potential.

It should be emphasized that we have not considered short-range three-body terms in the calculations. It follows from our analysis that this kind of interaction is not important at low densities; at low densities three-body collisions are obviously not probable. This point will be discussed in more detail in a forthcoming paper<sup>12</sup> by means of the triplet correlation function. It is important to mention that the potentials ( $v_2$  and  $v_3$ )

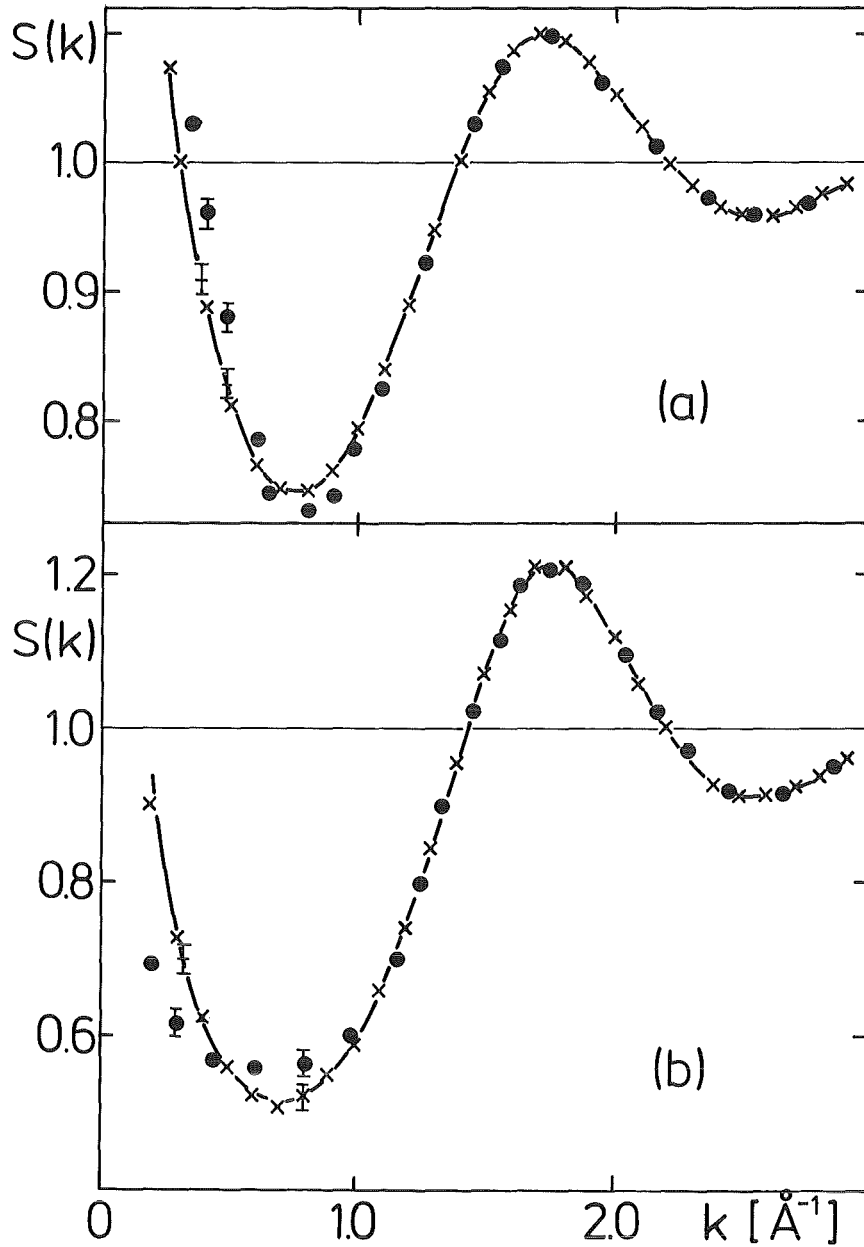


Fig. 1 Structure factor: (a)  $n = 2.884 \times 10^{27}$  atoms/m<sup>3</sup>,  
 (b)  $n = 6.19 \times 10^{27}$  atoms/m<sup>3</sup>; solid curve, MD results for  $\lambda=1$  (with error bars); full circles, MD results for  $\lambda=0$  (with error bars); crosses, experimental data (see Refs. 2 and 3). The experimental errors are smaller than 1%.

used in this study also give excellent agreement with the experimental crystal energies and pressures<sup>4,13</sup> and with phonon data<sup>14</sup>.

In Refs. 2 and 3 the analysis concerning the three-body-potential contribution have been done on the basis of the density expansion for the direct correlation function  $c(k)$  [see Ref. 2,

Eq. (2)], where  $c(k)$  is equal to  $[1 - S^{-1}(k)]/n$ . Using the experimental data for  $S(k)$  (see Ref. 3, Table I) we are able to check whether the density expansion is able to describe quantitatively well the structure data. If the density expansion [Ref. 2, Eq. (2)] is adequate, the quantity

$$C \equiv C_1(k,T) + C_2(k,T) = - \Delta c(k)/3\Delta n \quad (4)$$

should be independent of the density. However, it turned out that  $C$  varies strongly (examples for  $k = 0.4 \text{ \AA}^{-1}$  and  $T = 297 \text{ K}$  are given in Table I of this paper) and, therefore, we can conclude that the density expansion can only be valid if we average over a sufficiently large density range. It is shown in Ref. 2 (Fig. 3) that in this case the linear part of  $c(k)$  can be extracted; the higher-order terms ( $\rho^2, \rho^3, \dots$ ) are obviously cancelled if the data are averaged over a sufficiently large density range.

TABLE I Check of the density expansion. We used the same units for the density as in Ref. 3.

$S(0.4)$	$n$	$C$
1.010	0.520	0.0138
1.006	0.799	
0.870	3.160	0.0012
0.856	3.474	
0.667	5.65	0.0055
0.624	6.19	

#### IV. Dynamic Correlations

The complete information about the interaction between the particles of a many particle system can be extracted from static properties alone (see, for instance, Ref. 18). Because our MD model is able to describe very well the structure data of krypton gas, the MD model should also give reliable results for the dynamic correlation functions in that gas. Until now no experimental data were available for dynamic correlation functions. Therefore, the effects predicted here should be important for the construction of analytical models as well as serve as a guide for experimentalists.

In this section we show that we can construct measureable time correlation functions which are much more sensitive to three-body interactions than structure data.

##### IV.1 Density fluctuations

The fourier transform of the microscopic number density of a system with  $N$  krypton atoms having positions  $\vec{r}_j(t)$ ,  $j = 1, \dots, N$ , is given by

$$\rho_{\mathbf{k}}(t) = \frac{1}{N^{1/2}} \sum_{j=1}^N \exp[i\vec{k} \cdot \vec{r}_j(t)] \quad . \quad (5)$$

To describe density fluctuations, the correlation function (intermediate scattering function)

$$F(\mathbf{k}, t) = \langle \rho_{-\mathbf{k}}(0) \rho_{\mathbf{k}}(t) \rangle \quad (6)$$

is of interest. From this we obtain the coherent scattering law  $S(\mathbf{k}, \omega)$  by

$$S(\mathbf{k}, \omega) = \frac{1}{2\pi} \int_{-\infty}^{\infty} F(\mathbf{k}, t) \exp(i\omega t) dt. \quad (7)$$

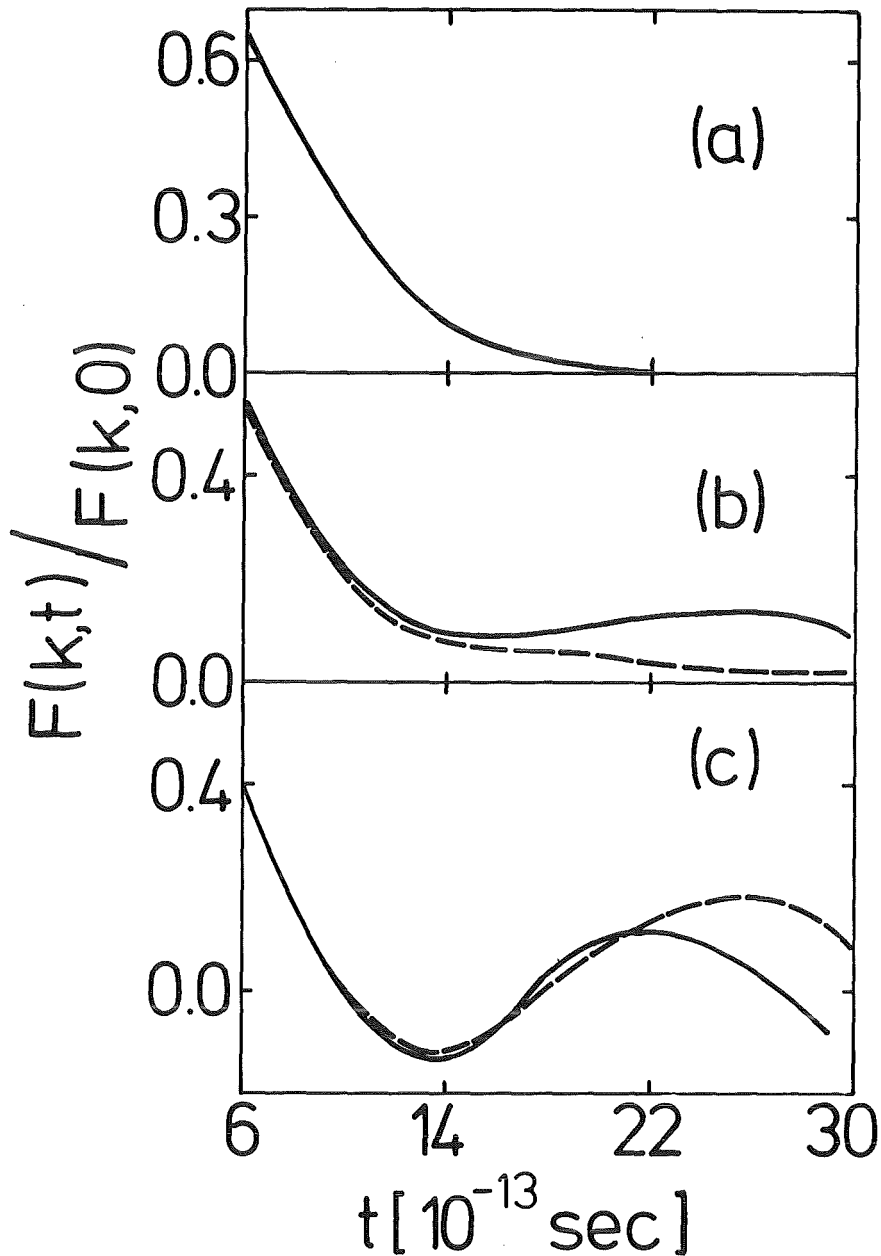


Fig. 2  $F(k,t)$ . (a) free gas, (b)  $n = 2.884 \times 10^{27}$  atoms/m<sup>3</sup>;  
 —  $\lambda=1$ , ----  $\lambda=0$ , (c)  $n = 6.19 \times 10^{27}$  atoms/m<sup>3</sup>; —  $\lambda=1$ ,  
 ----  $\lambda=0$ .

$S(k,\omega)$  is proportional to the coherent differential scattering cross section<sup>15</sup> and can be obtained from neutron scattering experiments.

A great deal of analytical models for  $S(k,\omega)$  have been listed and tested in Ref. 16. Testing of models using our MD data lies out of the scope of this paper. Here we only want to discuss some general features in connection with three-body interactions.

The effect due to  $v_3$  is more pronounced in  $F(k,t)$  than in  $S(k)$ . Examples are given in Fig. 2 for  $k = 1.1 \text{ \AA}^{-1}$ ; for this wave vector the three-body-potential contribution to  $S(k)$  is negligible. It can be seen from Fig. 2 that the three-body-potential contribution to  $F(k,t)$  is getting large with increasing time  $t$  (the statistical error is smaller than 1%). Such a tendency means that  $v_3$  will be most reflected in the low-frequency region of  $S(k,\omega)$ . However, the decay of  $F(k,t)$  with time is slow and the reliable determination of  $S(k,\omega)$  [see Eq. (7)] is only possible when  $F(k,t)$  is known for much larger time than was calculated and this can only be done by means of very large systems - larger than the systems used in this study. Because the long-time behavior of  $F(k,t)$  is too uncertain we hesitate to draw any conclusion for  $S(k,\omega)$  from the MD data.

Often-used models for the classical description of  $S(k,\omega)$  involve the knowledge of the even moments (see, for example, Ref. 16):

$$\bar{\omega}^n(k) \equiv \int_{-\infty}^{\infty} S(k,\omega) \omega^n d\omega, \quad n = 0, 2, 4, \dots \quad (8)$$

In particular, the moments up to four play an important role. Thus, in order to obtain a consistent picture we have not only to describe correctly  $S(k,\omega)$  but also  $\omega^n S(k,\omega)$ ,  $n = 2, 4$ . The function

$$R(k,\omega) = \omega^4 S(k,\omega) \quad (9)$$

is of considerable importance because  $\bar{\omega}^4(k)$  is the first moment which involves explicitly the interaction potential<sup>1</sup>.

MD results for  $R(k,\omega)$  and its Fourier transform

$$R(k,t) = \int_{-\infty}^{\infty} R(k,\omega) \exp(-i\omega t) d\omega = \frac{1}{N} \langle \ddot{p}_{-k}(0) \ddot{p}_k(t) \rangle \quad (10)$$

are shown in Figs. 3 and 4. In all cases the statistical error again is smaller than 1%. It can be seen that the effect of the

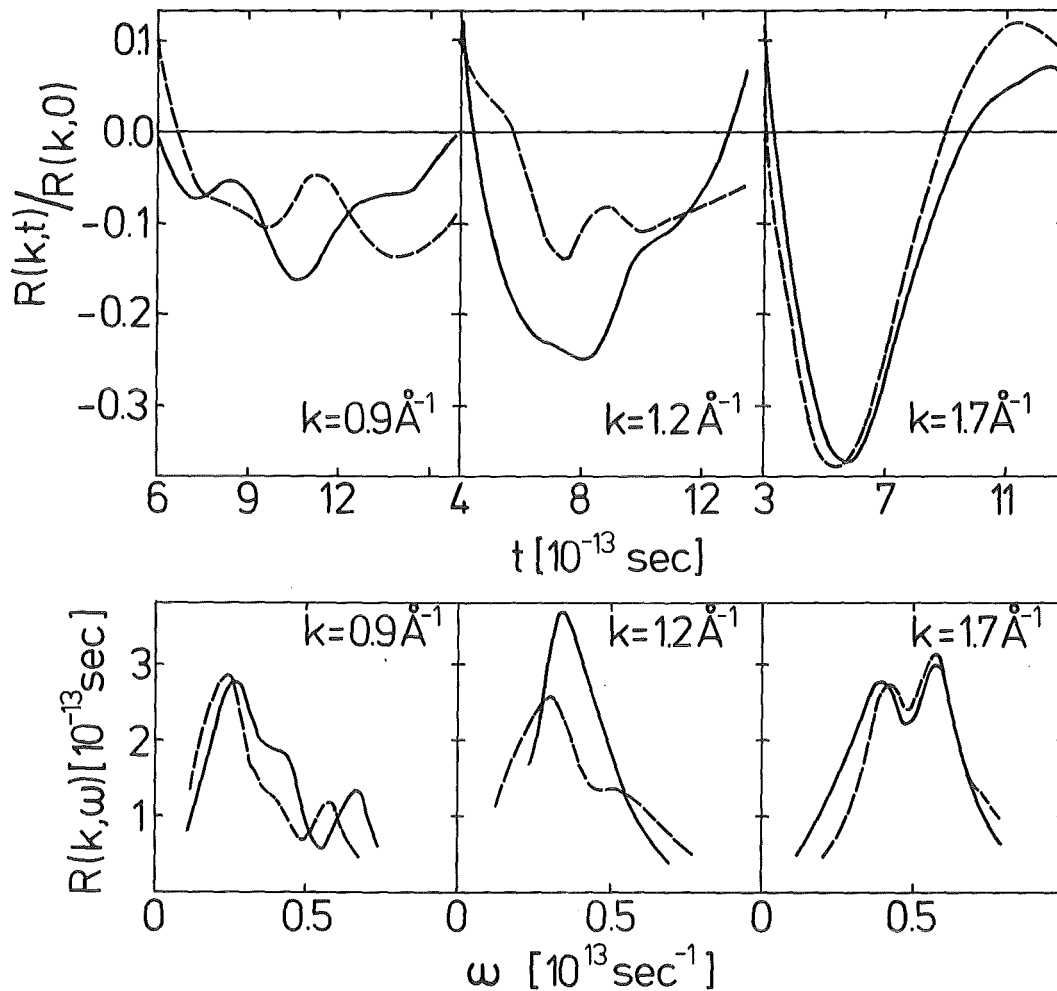


Fig. 3  $R(k,t)$  and  $R(k,\omega)$ ,  $n = 2.884 \times 10^{27}$  atoms/m<sup>3</sup>;  
 —  $\lambda=1$ , ----  $\lambda=0$ .

three-body interactions is relatively large.  $R(k,t)$  and  $R(k,\omega)$  are much more sensitive to three-body interactions than  $S(k)$  and  $F(k,t)$ ; the three-body-potential contribution to  $R(k,t)$  and its Fourier transform  $R(k,\omega)$  is about one order of magnitude larger than to  $S(k)$ .

The experimental determination of  $S(k,\omega)$  and  $R(k,\omega) = \omega^4 S(k,\omega)$  can be done with sufficient accuracy [as accurate as  $S(k)$ ] by neutron scattering experiments (see, for example, Ref. 17) and we expect that the ratio of error to effect for these functions is distinctly smaller than in the case of  $S(k)$ . Moreover, more experimental information can be obtained for  $R(k,\omega)$  than for  $S(k)$  since  $R(k,\omega)$  not only depends on  $k$  (as in the case of the structure factor) but also on  $\omega$ . Thus,  $R(k,\omega)$  is more qualified for the check

of three-body potentials than  $S(k)$ .

In summary, we can conclude that the function  $R(k, \omega)$  is of considerable interest for the following reasons.

(i) It forms an important model parameter (the fourth moment of the scattering law).

(ii) The three-body-potential contribution to  $R(k, \omega)$  is about one order of magnitude larger than to the structure factor.

(iii) The experimental determination of  $R(k, \omega)$  can be done with sufficient accuracy by neutron scattering experiments.

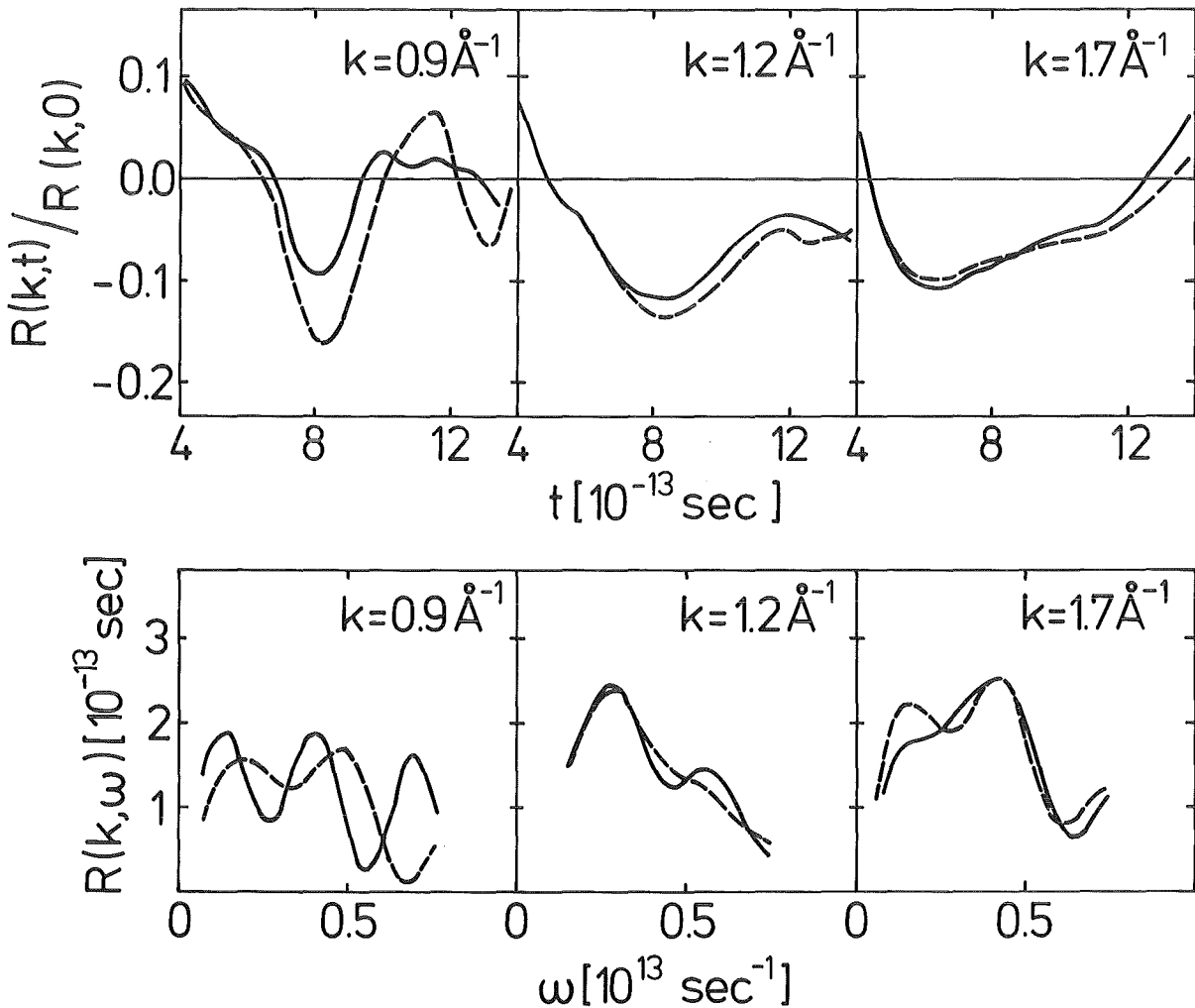


Fig. 4  $R(k,t)$  and  $R(k,\omega)$ ,  $n = 6.19 \times 10^{27}$  atoms/m $^3$ ;  
 —  $\lambda=1$ , ----  $\lambda=0$ .

## IV.2 Mean-square displacement

The auto-correlation function  $G_S(r,t)$  classically gives the probability that an atom at position  $r=0$  at time  $t=0$  is at position  $r$  at time  $t$ . The Fourier transform  $S_S(k,\omega)$  of  $G_S(r,t)$  can be measured by inelastic neutron scattering experiments.  $G_S(r,t)$  is related to  $S_S(k,\omega)$  by

$$G_S(r,t) = \int_{-\infty}^{\infty} dt d\vec{r} \exp[-i(\omega t + \vec{k} \cdot \vec{r})] S_S(k,\omega) \quad (11)$$

The mean-square displacement  $\langle r^2(t) \rangle$  can be obtained from  $G_S(r,t)$  without approximations by

$$\begin{aligned} \langle r^2(t) \rangle &= \left\langle \frac{1}{N} \sum_{i=1}^N [\vec{r}_i(t) - \vec{r}_i(0)]^2 \right\rangle \quad (12) \\ &= 2\pi \int_0^{\infty} dr r^2 G_S(r,t) , \end{aligned}$$

where  $\vec{r}_i(t)$  is the position of atom  $i$  at time  $t$ . MD results for  $\langle r^2(t) \rangle$  are represented in Fig. 5 (the statistical error is smaller than 1%). It can be seen from Fig. 5 that there are systematic deviations from the pair-theory values. In particular, we can conclude the following:

(i) The mobility of the atoms is smaller with the presence of three-body interactions.

(ii) The three-body-potential contribution is smaller in the case of  $n = 6.19 \times 10^{27}$  atoms/m<sup>3</sup>. This might be due to the fact that the repulsive part of the pair potential is getting effective with increasing density leading to less-pronounced three-body effects because the relative three-body-potential contribution is getting small.

We believe that the present experimental technique is sufficiently reliable (see, for example, Ref. 17) to allow quantitative comparison with our MD results for the mean-square displacement.  $\langle r^2(t) \rangle$  has already been extracted for liquid argon from neutron data<sup>19,17</sup>; the experimental results for the

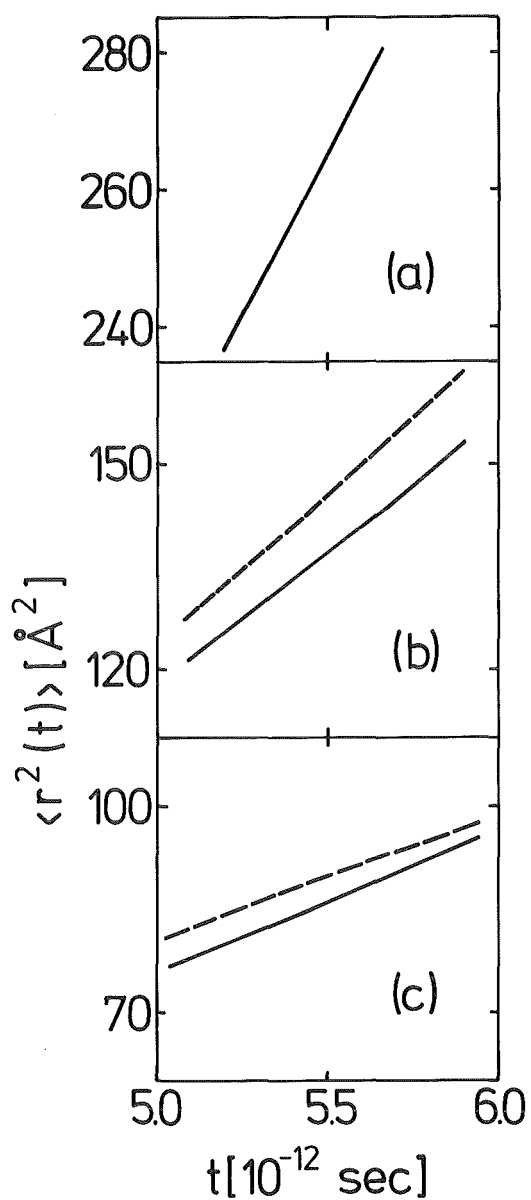


Fig. 5 Mean-square displacement (a) free gas, (b)  $n = 2.884 \times 10^{27}$  atoms/ $m^3$ ; —  $\lambda=1$ , ---  $\lambda=0$ , (c)  $n = 6.19 \times 10^{27}$  atoms/ $m^3$ ; —  $\lambda=1$ , ---  $\lambda=0$ .

double-differential scattering cross section have been Fourier transformed and it was possible to determine  $G_s(r,t)$  and  $\langle r^2(t) \rangle$ .

## V. Asymptotic time behavior of the velocity auto-correlation function

### V.1 General remarks

The principal difficulty in calculating transport coefficients (self-diffusion coefficient, heat conductivity, etc.) concerns the estimation of the asymptotic time behavior of correlation functions; the Green-Kubo formulas express the transport coefficients as integrals over corresponding time correlation functions. In the case of the self-diffusion coefficient  $D$  the velocity auto-correlation function (VAF) is the relevant time correlation function and we have

$$D \sim \int_0^{\infty} \psi(t) dt \quad , \quad (13)$$

where  $\psi(t)$  is the VAF which is defined by

$$\psi(t) = \langle \vec{v}(0) \cdot \vec{v}(t) \rangle / \langle v(0)^2 \rangle \quad (14)$$

$\vec{v}(t)$  is the velocity at time  $t$  for one atom of the ensemble and the brackets  $\langle \dots \rangle$  denote a statistical average.  $\psi(t)$  can be determined very accurately by means of molecular-dynamics (MD) because in this case an independent calculation may be performed for each of the  $N$  particles in the system.

The asymptotic time behavior of the VAF has already been investigated by MD for hard spheres by Alder and Wainwright<sup>20,21</sup> and for a fluid of soft repulsive particles by Levesque and Ashurst<sup>22</sup>. Both studies led to the famous  $t^{-3/2}$  decay of the VAF for three-dimensional systems, and this law has also been deduced analytically by a great variety of apparently different starting points (see, for example, Refs. 23, 24 and 25).

In Refs. 20, 21 and 22 only short-range (repulsive) potentials have been used for the study of the long-time tail of the VAF. Till now the  $t^{-3/2}$  law of the VAF has not yet been verified by MD on the basis of short-range and long-range interactions

although it is widely accepted that the dynamical properties of a system are considerably influenced by the long-range part of the pair potential (see, for example, Ref. 26), in particular, its effect on the VAF seems to be getting large with increasing time<sup>27</sup>. Moreover, not only the pair potential is distinctly reflected in time correlation functions but also three-body interactions. This has been demonstrated in Refs. 1 and 9; it turned out that (as in the case of the long-range part of the pair potential) the effects due to three-body forces on  $\psi(t)$  also seems to be getting large with increasing time (see Fig. 3 of Ref. 1). In conclusion, it is quite questionable whether the asymptotic time behavior of  $\psi(t)$  is completely described by short-range interactions alone.

In this section we want to investigate by means of MD the long-time tail of the VAF for the realistic krypton many-particle system described in section II. In contrast to the studies represented in Refs. 20, 21 and 22, not only the short-range part of the pair potential but also its long-range part and three-body interactions have been considered.

## V.2 Estimation of the time-region

The MD results are only valid<sup>29</sup> for times  $t < T = L/c$ , where  $L$  is again the size of the box and  $c$  is the velocity of sound in the system; for times  $t < T$  the boundary conditions should have no influence on the VAF. In the case of gaseous krypton at the density  $n = 2.884 \times 10^{27}$  atoms/m<sup>3</sup> ( $n = 6.19 \times 10^{27}$  atoms/m<sup>3</sup>) the characteristic time  $T$  takes the value  $9.5 \times 10^{-12}$  sec ( $6.5 \times 10^{-12}$  sec).

With such a model we were able to observe  $\psi(t)$  within a time-region which is equivalent to that in Ref. 22 (soft repulsive potential simulation). The time scale in Ref. 22 is given in units of

$$h = 0.032 \quad \left( \frac{m\sigma^2}{48\epsilon} \right)^{1/2} ,$$

where  $\sigma$  and  $\epsilon$  are the pair potential parameter and  $m$  is the mass of an atom. Using for  $m$ ,  $\sigma$  and  $\epsilon$  the data of krypton (see Ref. 4) we obtained:

$$h = 1.1 \times 10^{-14} \text{ sec} .$$

In the case of  $n = 2.88 \times 10^{27}$  atoms/m<sup>3</sup> the time-region is

$$0 \leq t \leq 9.5 \times 10^{-12} \text{ sec} .$$

Or in units of  $h$ :

$$0 \leq t \leq 860$$

The time-region in Ref. 22 (Table I) is (also in units of  $h$ )

$$0 \leq t \leq 780$$

Therefore, we can conclude that the time-region of our calculation is of the same order as in Ref. 22.

### V.3 Results and Discussion

First we have investigated the influence of the three-body forces on the microscopic time behavior of the atoms within the time region of  $3.6 \times 10^{-12} \text{ sec} < t < T$ ; we shall see below that this time region is important for the determination of the long-time tail of the VAF. For this purpose we have calculated the square forces  $F_i^2(t)$ ,  $i=1, \dots, N$ , with and without the presence of three-body interactions. Typical examples are represented in the Figs. 6 and 7. Although all atoms were in exactly the same state (positions

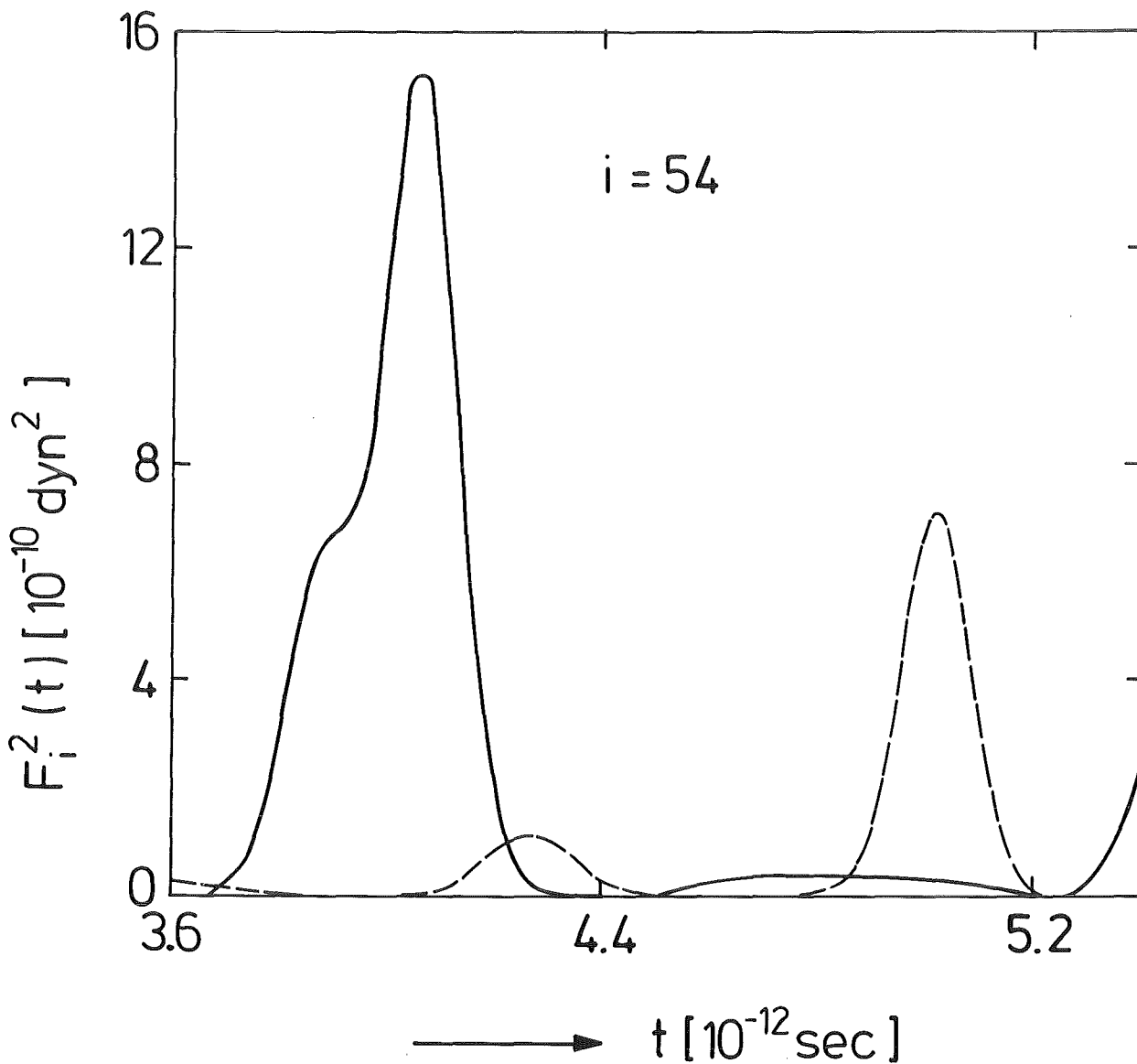


Fig. 6 Microscopic square forces  $\vec{F}_i^2(t)$  for the density  $n = 2.884 \times 10^{27} \text{ atoms/m}^3$  and particle 54. — with the presence of  $v_3$ , ---- without the presence of  $v_3$ .

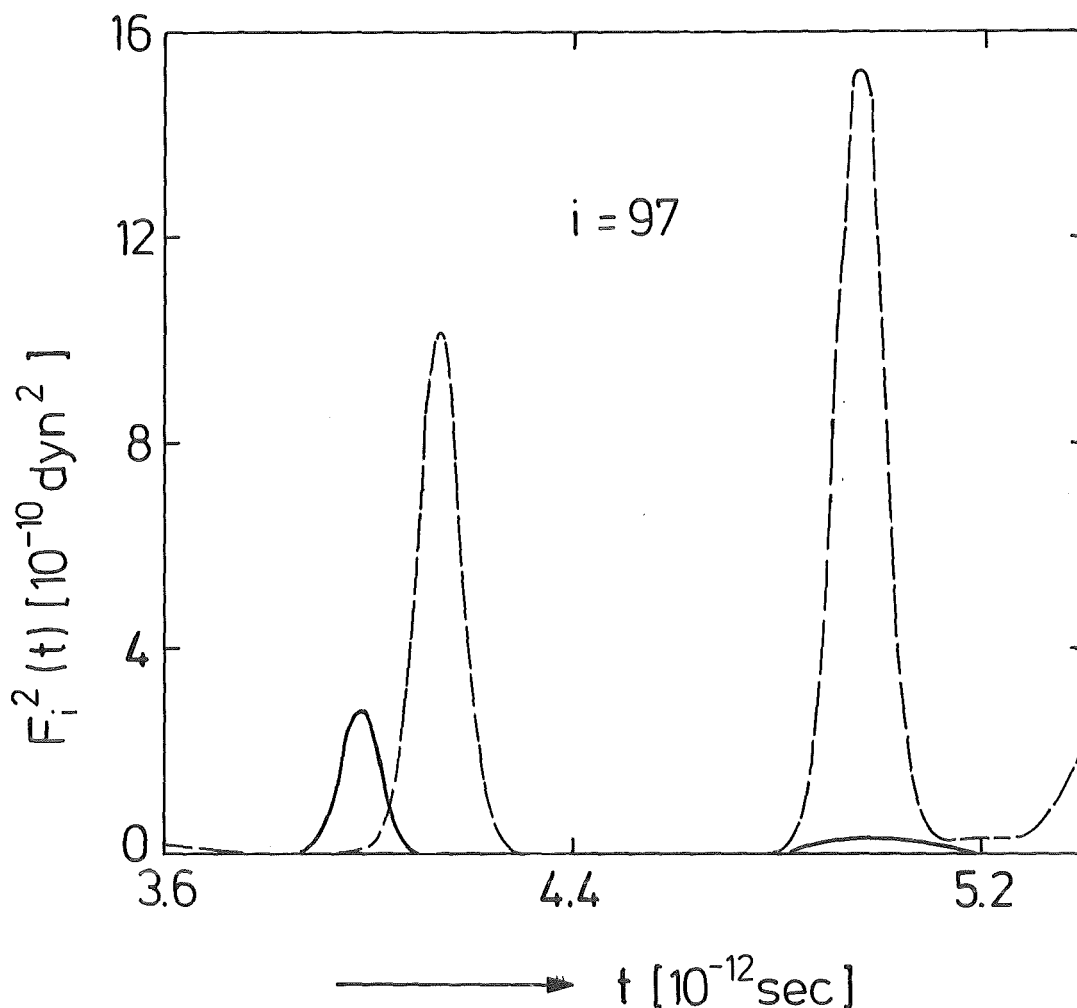


Fig. 7 Microscopic square forces  $\vec{F}_i^2$  for the density  $n = 2.884 \times 10^{27}$  atoms/m<sup>3</sup> and particle 97. — with the presence of  $v_3$ ; ---- without the presence of  $v_3$ .

and velocities) at  $t=0$ , it can be seen from the Figs. 6 and 7 that the temporal sequences of attractive and repulsive forces acting on the atoms are quite different from each other; in other words, the microscopical behavior of the atoms is strongly influenced by the three-body forces.

Figs. 8, 9, 10 and 11 show the results for the VAF. In all cases, the statistical error<sup>30</sup> of  $\psi(t)$  is smaller than 1%. From Figs. 8, 9, 10 and 11 we observe the following:

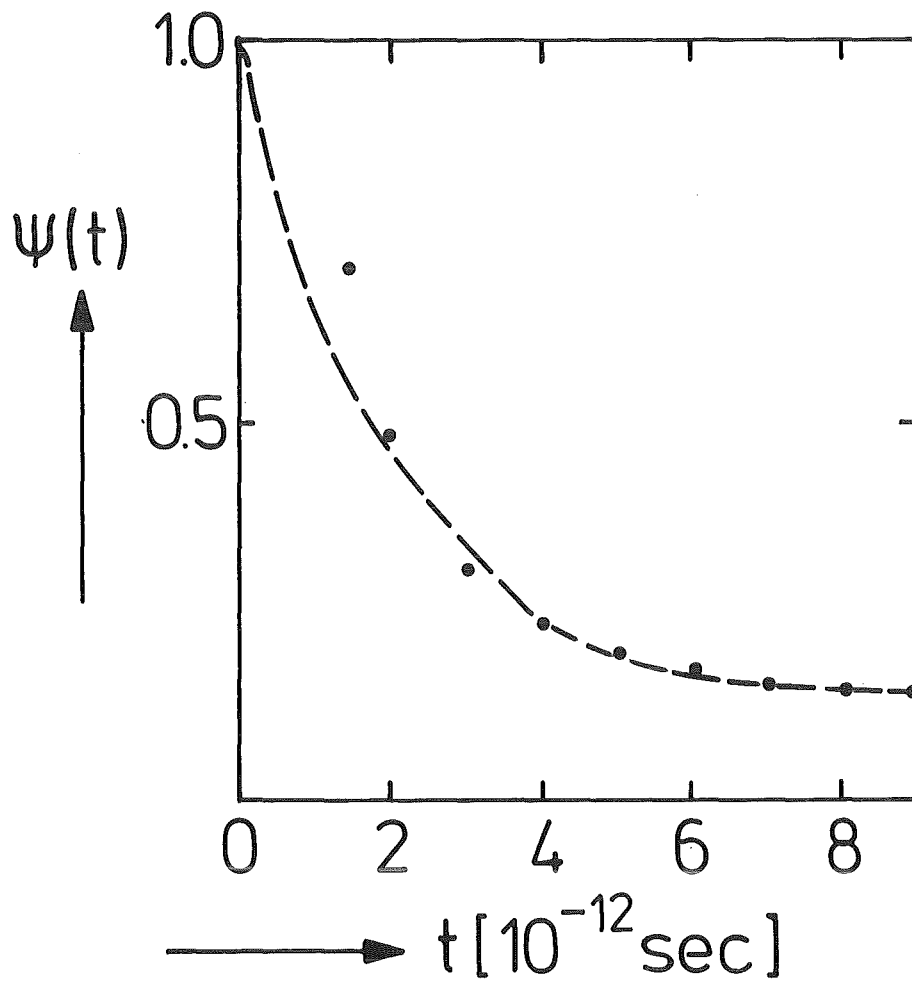


Fig. 8 VAF for the density  $n = 2.884 \times 10^{27}$  atoms/m<sup>3</sup>  
 ---- without the presence of  $\nu_3$ ;  $\cdots \psi(t) = \alpha_0 t^{-3/2} + \beta_1$

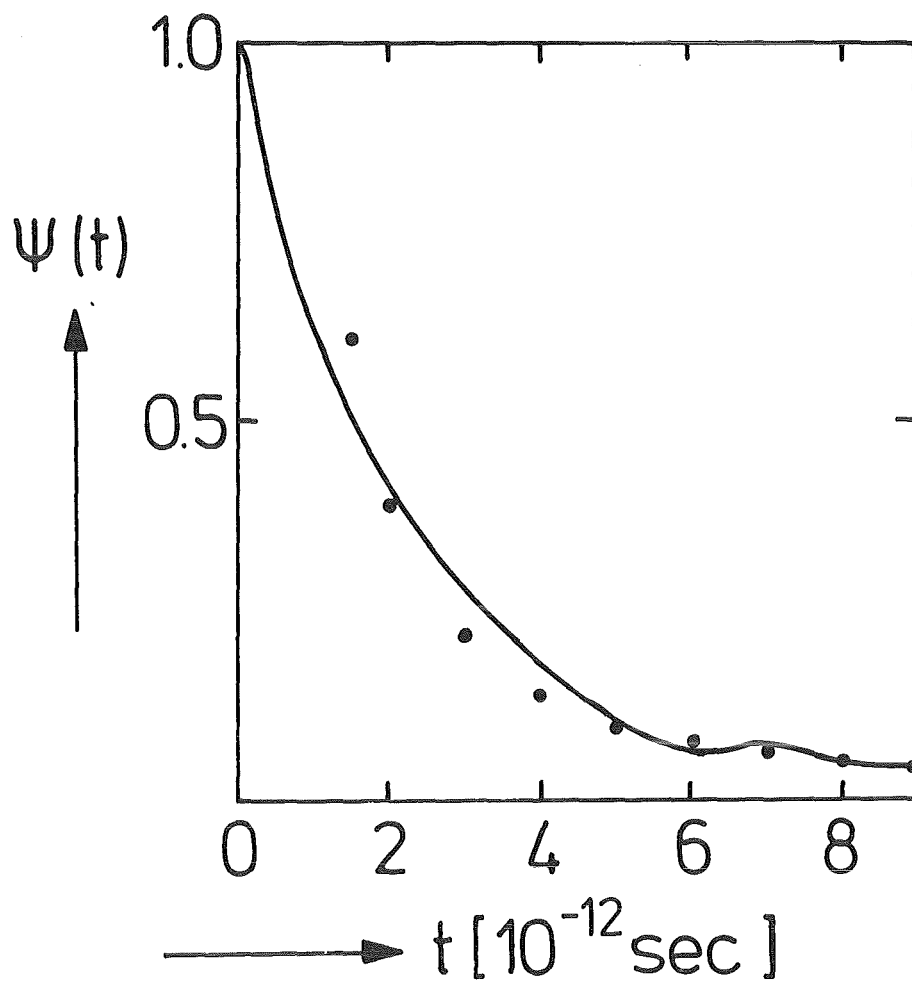


Fig. 9 VAF for the density  $n = 2.884 \times 10^{27}$  atoms/m<sup>3</sup>  
 — with the presence of  $\nu_3$ ;  $\cdots \psi(t) = \alpha_0 t^{-3/2}$

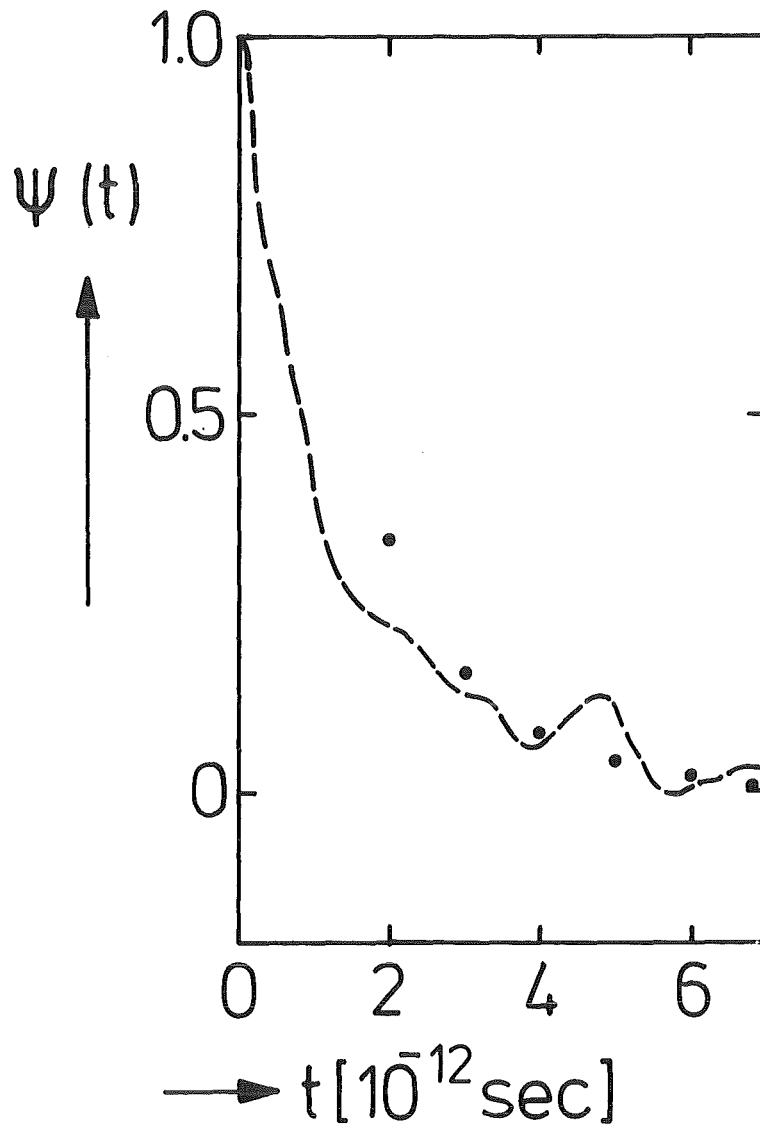


Fig. 10 VAF for the density  $n = 6.19 \times 10^{27}$  atoms/m<sup>3</sup>  
 ---- without the presence of  $\nu_3$ ; .....  $\psi(t) = \alpha_0 t^{-3/2} + \beta_2$

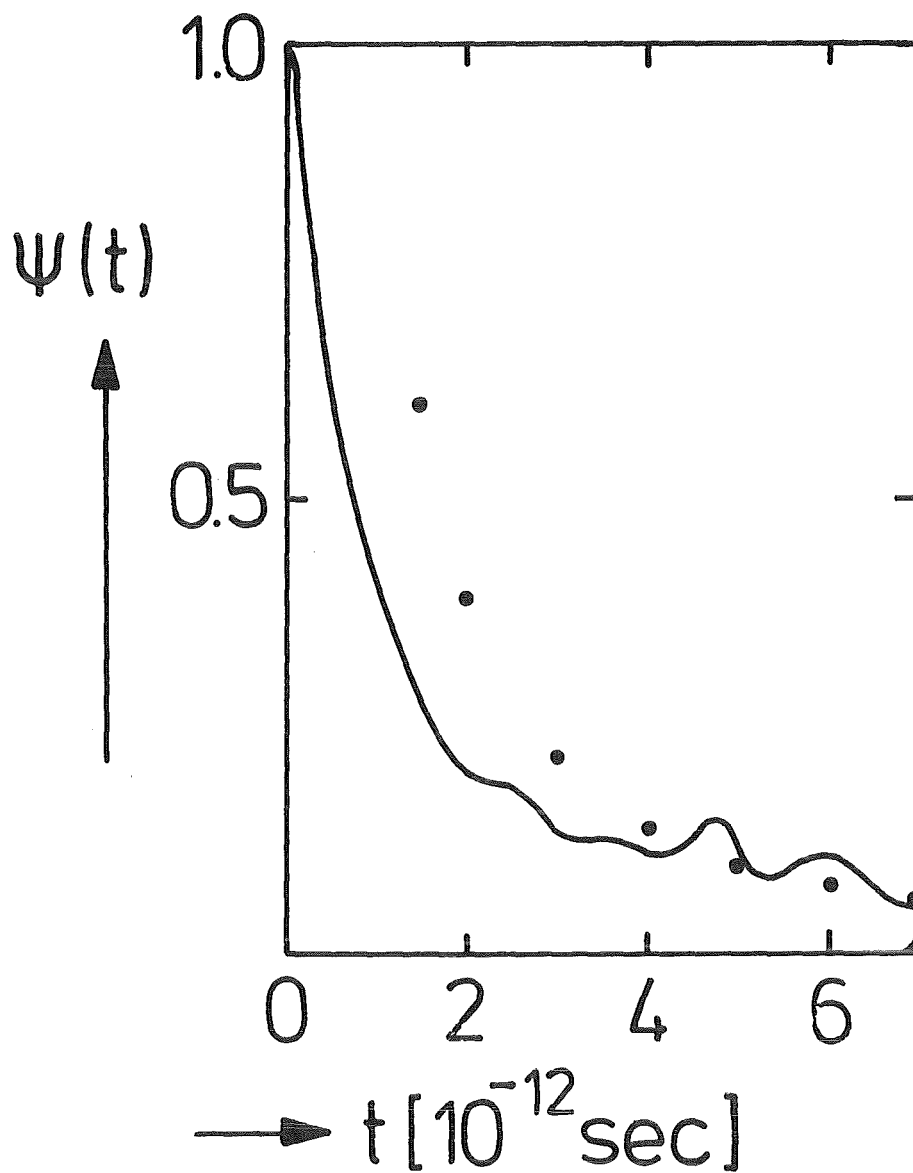


Fig. 11 VAF for the density  $n = 6.19 \times 10^{27}$  atoms/m<sup>3</sup>  
 — with the presence of  $\nu_3$ ;  $\dots \psi(t) = \alpha_0 t^{-3/2}$

(1) It can be seen that the effects due to the three-body interactions  $v_3$  are not so significant in the correlation function  $\psi(t)$  (it is formed by averaging over  $N$  independent calculations) as we have found for the microscopic time behavior of the particles (Figs. 6 and 7); at first glance the curves without  $v_3$  are similar to those with  $v_3$ . However, there are systematic deviations due to  $v_3$ . It can be seen that these deviations are relatively large within the time-region of interest. For example, in the case of  $n = 2.884 \times 10^{27}$  atoms/m<sup>3</sup> (Figs. 8 and 9) the pair-theory value at  $t = 6 \times 10^{12}$  sec is about three times (300%) larger than the  $v_3$ -dependent value.

(2) In contrast to Figs. 8 and 9, in Figs. 10 and 11 a small oscillatory component is observed in the long-time tail which is greater than the errors; this is obviously a density-effect.

(3) We know from Ref. 22 that  $\psi(t)$  for a system consisting of soft repulsive particles (only the short-range part of the pair potential  $v_2$  has been considered) decays like  $t^{-3/2}$ . Figs. 8 and 10 show (both, the short-range and the long-range part of  $v_2$  are considered in the calculation) that the  $t^{-3/2}$  term is superimposed by an additional term which seems to be slowly varying in time and is approximated in Figs. 8 and 10 by the constants  $\beta_1$  and  $\beta_2$ , respectively. However, it can be seen from Figs. 9 and 11 that with the presence of  $v_3$  (and of course with the full pair potential) a pure  $t^{-3/2}$  law is observed; the small oscillations at the density  $n = 6.19 \times 10^{27}$  atoms/m<sup>3</sup> are not important for this discussion because they appear as well with  $v_3$  as without  $v_3$ .

In order to decide whether the asymptotic region  $\psi(t)$  has been reached we have analyzed our MD data by means of a well known sum rule of the force correlation function  $f(t) = \langle \vec{F}(0) \cdot \vec{F}(t) \rangle$  ( $\vec{F}(t)$  is the force at time  $t$  for one atom of the ensemble):

$$\int_0^{\infty} \langle \vec{F}(0) \cdot \vec{F}(t) \rangle dt = 0 \quad (16)$$

The integral from 0 to  $\tau$  ( $\tau$  is the limiting time in our MD calculations) has been calculated by means of the MD data using the individual forces. In the region from  $\tau$  to  $\infty$ ,  $f(t)$  has been expressed by the laws for the long-time tails of  $\psi(t)$  (in the case with  $v_3: \alpha_0 t^{-3/2}$ ) using the well known identity  $f(t) = -3 k_B T m \ddot{\psi}(t)$ . It follows that

$$A = \int_{\tau}^{\infty} f(t) dt = \frac{-9 k_B T m}{2} \alpha_0 \tau^{-5/2} \quad (17)$$

So, if the asymptotic region has been reached, the integration of our MD data for  $f(t)$  from 0 to  $\tau$  must be identical to  $-A$ ; this follows directly from the general expression (16). A careful analysis of our data showed that this is definitely fulfilled in the calculation with  $v_3$  (Figs. 8 and 10). Thus, only in the calculation with  $v_3$  the asymptotic region has been reached. Clearly, this behavior can lead to large effects in the diffusion coefficient  $D$  because the Green-Kubo integral (see Eq. 14) is formed from 0 to  $\infty$ .

The long-time tails in Figs. 9 and 11 start approximately at  $t = 4 \times 10^{-12}$  sec corresponding to 5 - 6 two-body collisions; two-body collisions take place at distances where the repulsive part of  $v_2$  is effective (in our case at distances smaller than 4 Å). In Ref. 22 much more collisions ( $\sim 18$ ) are needed in order to reach the asymptotic region. However, the calculation in Ref. 22 has been done without  $v_3$ , and  $v_3$  can be repulsive at large distances<sup>5</sup>. Thus, in the calculation with  $v_3$  the two-body collisions are superimposed by "long-distance collisions", and this is obviously the reason why the asymptotic region is reached after a relatively short time.

Pomeau showed<sup>31</sup> that  $\psi(t)$  can be generally expressed by an infinite serie with the terms  $t^{-3/2}$ ,  $t^{-7/4}$ , ... . Within the time region of  $4 \times 10^{-12}$  sec  $< t < 9 \times 10^{-12}$  sec the  $t^{-3/2}$  law is obviously fulfilled (see Fig. 9); all the other terms ( $t^{-7/4}$ , ...) are negligible. Because the exponents of all the higher order terms are larger than 3/2, we can conclude that also for

$9 \times 10^{-12} \text{ sec} < t < \infty$  the terms with  $t^{-7/4}$ , ... do not contribute to  $\psi(t)$ . Also from this point of view it is justified to state that we observe the asymptotic long-time tail of  $\psi(t)$  in our calculation. It should be mentioned that our results for the diffusion coefficients (using the  $t^{-3/2}$  law) are also supported by recent neutron scattering data<sup>32</sup>.

(4) The value of the prefactor  $\alpha_0$  of the  $t^{-3/2}$  law is  $1.15 \times 10^{-18} \text{ sec}^{3/2}$ . In all calculations we did not find that  $\alpha_0$  is dependent on the density and on  $v_3$ , respectively. A number of other methods<sup>25</sup> (kinetic theory, generalized Landau-Placzek theory, hydrodynamics) lead also to the conclusion that  $\psi(t)$  decrease for large times like  $t^{-3/2}$ . For example, within the kinetic theory the prefactor of the  $t^{-3/2}$  law is given by<sup>24</sup>

$$\alpha_D = \alpha_{D,0}\rho^2 + \alpha_{D,1}\rho^3 + \dots \quad , \quad (18)$$

where  $\rho = na^3$ ;  $a$  is the diameter of the particle. Ernst<sup>23</sup> et al. restricted themselves on a hydrodynamical description and found that in this case the prefactor is given by the first term of Eq. (18):  $\alpha_D = \alpha_{D,0}\rho^2$ . Without going in detail, it is easy to show that this hydrodynamical theory is not able to describe our prefactor  $\alpha_0$ ; it turned out that  $\alpha_0$  is at least 4.25 times larger than  $\alpha_{D,0}\rho^2$  (first term of Eq. (18)). We obviously have to consider more than one term in the infinite serie of the density expansion (18). It should be mentioned that also the experimental structure data of our krypton system cannot be described quantitatively if we restrict ourselves on the first terms in the density expansion of the direct correlation function (see Table I); also here the higher order-terms in the density expansion are not small compared with the first term of the infinite serie.

The hydrodynamical theory<sup>23</sup> ( $\alpha_D = \alpha_{D,0}\rho^2$ ) is not valid in the critical region and we believe that the reason for the deviations between  $\alpha_0$  and  $\alpha_{D,0}\rho^2$  might be due to the critical behavior which we observe for both densities (the critical density is  $6.5 \times 10^{27}$  atoms/m<sup>3</sup>) indicated by an increase of the structure factor  $S(k)$

at low  $k$  (see Fig. 1). The anomalous increase in the life-time of time correlations<sup>33</sup> associated with critical fluctuations supports this assumption; clearly, an increase of the prefactor  $\alpha_0$  means an increase in the life-time of the velocity correlations. It should be emphasized that the short-range (repulsive) part of the pair potential alone cannot describe the typical features of critical fluctuations<sup>34</sup> and it is therefore not surprising that the prefactor of the  $t^{-3/2}$  law of a system consisting of soft particles<sup>22</sup> is compatible with  $\alpha_{D,0} \rho^2$  which - as already remarked above - also does not involve critical fluctuations.

(5) The Fourier transform of  $\psi(t)$  is the frequency spectrum  $f(\omega)$  which is in the case of the harmonic solid the frequency spectrum of the normal modes.  $f(\omega)$  can be determined experimentally by neutron diffraction experiments using an extrapolation procedure<sup>35</sup>:

$$f(\omega) = \frac{2m}{k_B T} \lim_{Q \rightarrow 0} \frac{S_S(Q, \omega)}{Q^2} \quad (19)$$

$S_S(Q, \omega)$  is the incoherent dynamic structure factor. The frequency spectrum  $f(\omega)$  is connected to the VAF by

$$f(\omega) = \frac{2}{\pi} \int_0^{\infty} \psi(t) \cos \omega t \, dt \quad , \quad (20)$$

where  $f(\omega)$  is normalized to unity:

$$\int_0^{\infty} f(\omega) \, d\omega = 1 \quad (21)$$

In order to obtain reliable results for  $f(\omega)$  we have extrapolated our MD data for  $\psi(t)$ , which are given in the Figs. 9 and 11, by means of the  $t^{-3/2}$  law. Figs. 12 and 13 show the results for the frequency spectrum in the case with  $v_3$ . The MD results for the calculations without  $v_3$  (see Figs. 8 and 10) have not been transformed because in these calculations the asymptotic time region seems not to be reached.

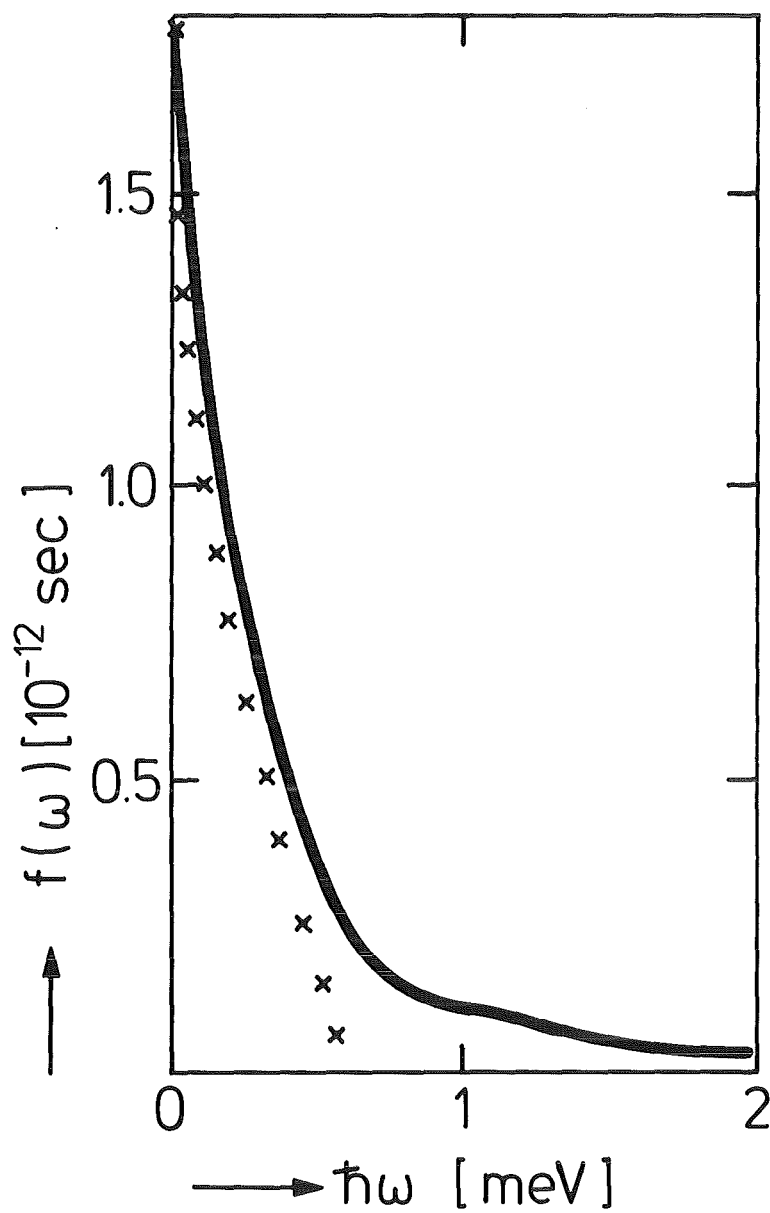


Fig. 12  $f(\omega)$  for the density  $n = 2.884 \times 10^{27}$  atoms/m<sup>3</sup>  
 — MD data (extrapolated by the  $t^{-3/2}$  law)  
 x x x Eq. 24

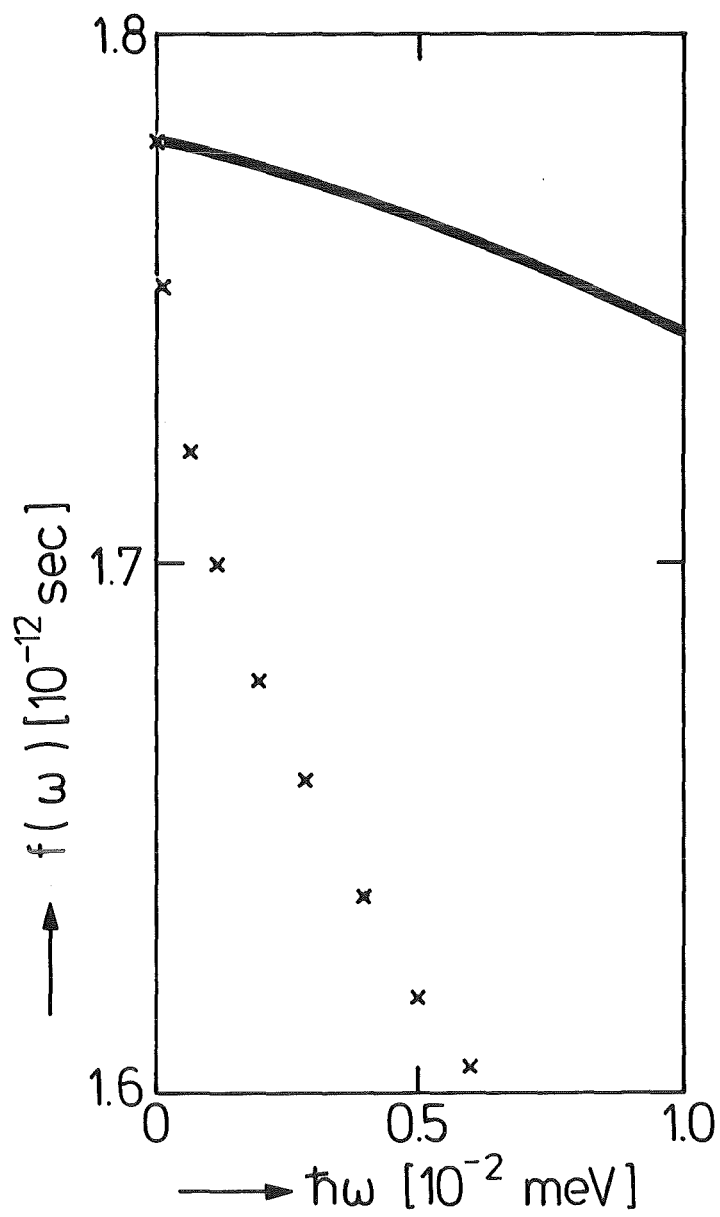


Fig. 13  $f(\omega)$  for the density  $n = 6.19 \times 10^{27}$  atoms/m<sup>3</sup>  
 — MD data (extrapolated by the  $t^{-3/2}$  law)  
 x x x Eq. (24)

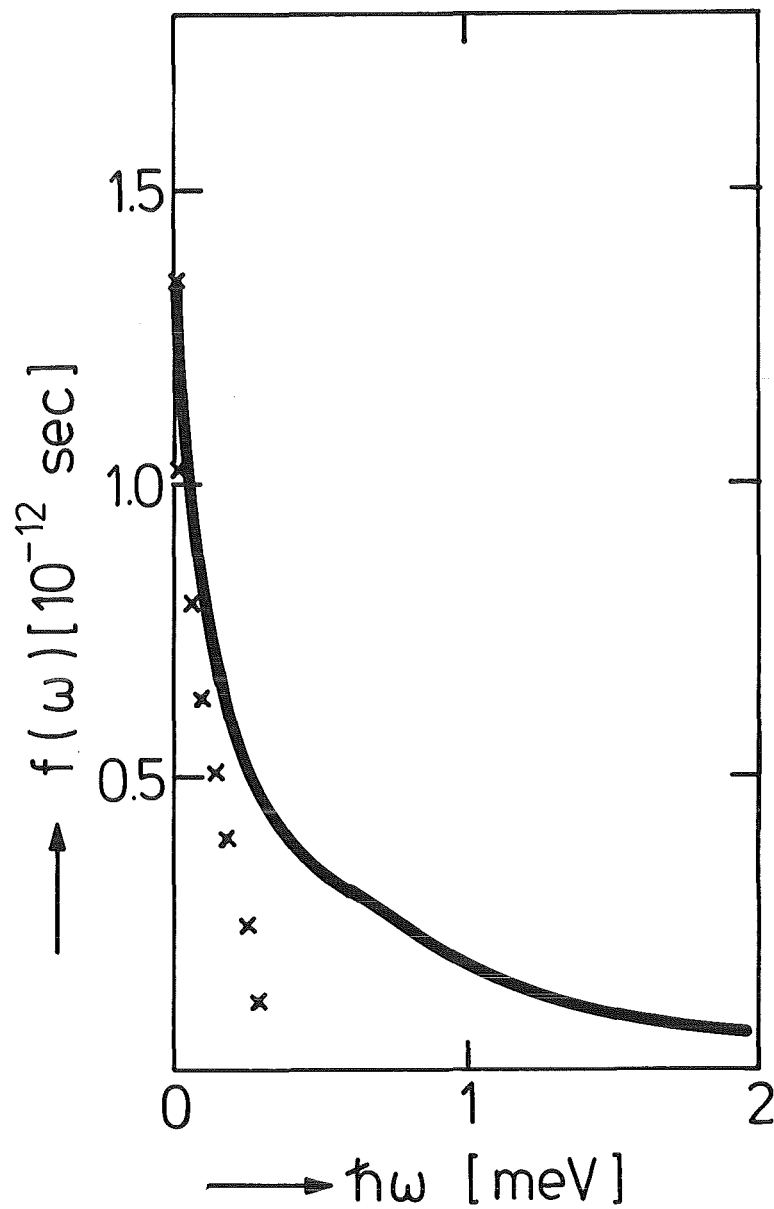


Fig. 14  $f(\omega)$  at very small frequencies ( $n = 2.884 \times 10^{27}$  atoms/m<sup>3</sup>)

— MD data (extrapolated by the  $t^{-3/2}$  law)

x x x Eq. (24)

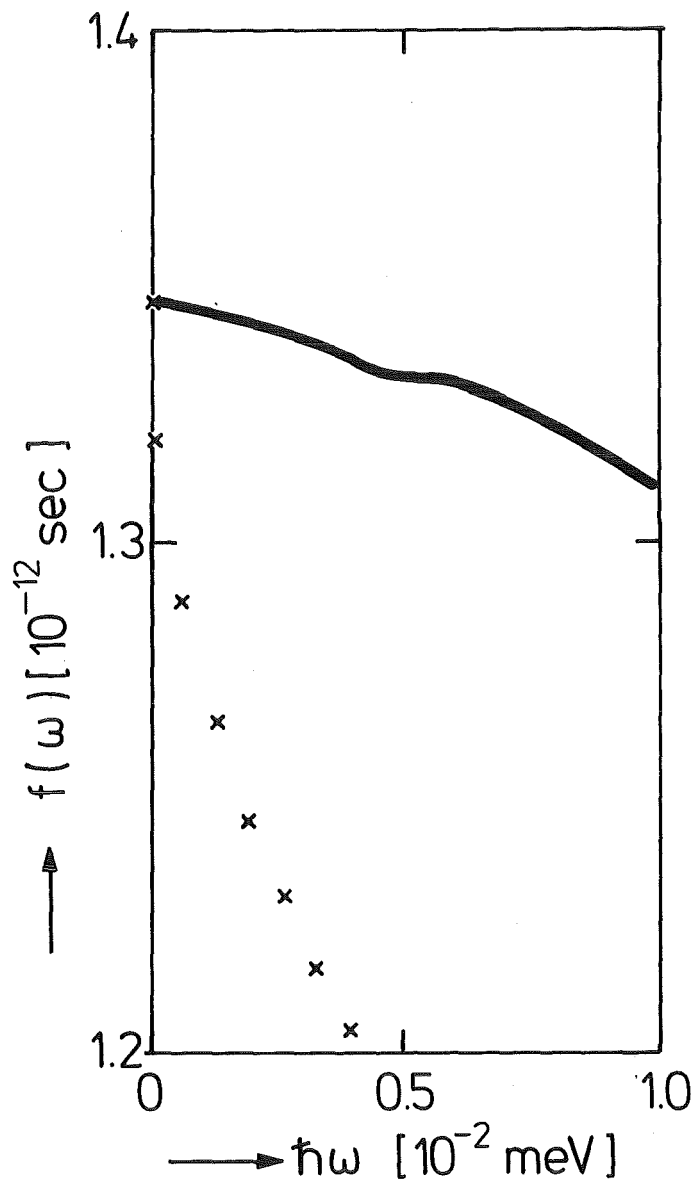


Fig. 15  $f(\omega)$  at very small frequencies ( $n = 6.19 \times 10^{27}$  atoms/m<sup>3</sup>)

— MD data (extrapolated by the  $t^{-3/2}$  law)

x x x Eq. (24)

The frequency-dependence of  $f(\omega)$  for a free gas is described by a deltafunction:  $f(\omega) \sim \delta(\omega)$ . As can be seen from the Figs. 12 and 13 also our results are strongly peaked at  $\omega = 0$ . In particular, in the case of  $n = 2.884 \times 10^{27}$  atoms/m<sup>3</sup> the free-gas-characteristics are more pronounced than in the case of  $n = 6.19 \times 10^{27}$  atoms/m<sup>3</sup>.

Gaskell and March<sup>36</sup> assumed that for  $f(\omega)$  an expansion in  $\omega^{1/2}$  around  $\omega = 0$  exists:

$$f(\omega) = f(0) + a_1 \omega^{1/2} + a_2 \omega + a_3 \omega^{3/2} + \dots \quad (22)$$

Using  $\psi(t) = \alpha_0 t^{-3/2}$  and Eq. (20) it is straightforward to show that the  $t^{-3/2}$  law produces a term in  $f(\omega)$  which is proportional to  $\omega^{1/2}$ . Thus, the leading term in Eq. (22) should be  $a_1 \omega^{1/2}$  and the coefficient  $a_1$  is given by

$$a_1 = -\sqrt{\frac{8}{\pi}} \alpha_0 \quad (23)$$

Figs. 12 and 13 show that the shape of  $f(\omega)$  in the vicinity of  $\omega = 0$  is well approximated by

$$f(\omega) = f(0) - \sqrt{\frac{8}{\pi}} \alpha_0 \omega^{1/2} \quad (24)$$

However, we do not observe a cusp and a negatively infinite slope of  $f(\omega)$  at  $\omega = 0$  as predicted by the Eqs. (22) and (24); this conclusion has been drawn from the Figs. 14 and 15 which show  $f(\omega)$  at very small frequencies. The reason for this behavior is obviously due to the fact that the  $t^{-3/2}$  law is not valid for the whole time region ( $0 \leq t \leq \infty$ );  $\psi(t)$  deviates strongly from the  $t^{-3/2}$  law at small times obviously compensating the negatively infinite slope of  $f(\omega)$  at  $\omega = 0$  due to Eq. (24).

## VI. Summary

Molecular dynamics calculations on krypton gas at 297 K have been performed taking into account three-body interactions. The purpose of this paper was to show the following:

(i) The experimental structure data can be well described if we use for the three-body potential the Axilrod-Teller form; the potentials used in this study also give excellent agreement with the experimental crystal energies and pressures<sup>4,13</sup> and with phonon data<sup>14</sup>.

(ii) The three-body-potential contribution to dynamic correlations is about one order of magnitude larger than that to static correlations. The experimental determination of the dynamic correlation functions can be done with sufficient accuracy by neutron-scattering experiments and we expect that the ratio of error to effect for these functions is smaller than in the case of the structure factor. It would be most fruitful to perform neutron-scattering experiments and to compare the results with those predicted here.

(iii) The asymptotic time behavior of the velocity autocorrelation function has been investigated. It turned out that the long-time tail is strongly influenced by three-body forces. The famous  $t^{-3/2}$  law has been observed in the calculation with the presence of three-body forces.

Our next step is to systematically investigate three-body effects as a function of density. In particular, we shall investigate the influence of short-range three-body terms on atomic correlations which were obviously not important in the low-density case discussed here.

References

- <sup>1</sup>W. Schommers, Phys. Rev. A 16, 327 (1977).
- <sup>2</sup>P.A. Egelstaff and A. Teitsma, Phys. Rev. Lett. 43, 503 (1979).
- <sup>3</sup>A. Teitsma and P.A. Egelstaff, Phys. Rev. A 21, 367 (1980).
- <sup>4</sup>J.A. Barker et al., J. Chem. Phys. 61, 3081 (1979).
- <sup>5</sup>B.M. Axilrod and E. Teller, J. Chem. Phys. 11, 229 (1943).
- <sup>6</sup>M.L. Klein and J.A. Venables, in Rare Gas Solid (Academic, New York, 1977).
- <sup>7</sup>J.A. Barker et al., Mol. Phys. 21, 657 (1971).
- <sup>8</sup>A. Rahmann, Phys. Rev. 136, A 405 (1964).
- <sup>9</sup>W. Schommers, Ges. Kernforschung, KfK 1489 (1972).
- <sup>10</sup>R. Zwanzig and N. Ailawadi, Phys. Rev. 182, 280 (1969).
- <sup>11</sup>N. Ailawadi, Phys. Rev. A 5, 1968 (1972).
- <sup>12</sup>W. Schommers (unpublished).
- <sup>13</sup>D.N. Card and P.W. Jacobs, Mol. Phys. 34, 1 (1977).
- <sup>14</sup>J.A. Barker, M.L. Klein, and M.V. Bobetic, IBM J. Res. Dev. 20, 222 (1976).
- <sup>15</sup>L. van Hove, Phys. Rev. 95, 249 (1954).
- <sup>16</sup>J.M. Rowe and K. Sköld, Neutron Inelastic Scattering (IAEA, Vienna, 1972), p. 413.
- <sup>17</sup>K. Sköld et al., Phys. Rev. A 6, 1107 (1972).
- <sup>18</sup>A. Münster, Statistical Thermodynamics (Springer, New York, 1969).
- <sup>19</sup>B. Dasannacharya and K. Rao, Phys. Rev. A 137, 417 (1965).
- <sup>20</sup>B.J. Alder, T.E. Wainwright, Phys. Rev. Lett. 18, 988 (1967).
- <sup>21</sup>B.J. Alder, T.E. Wainwright, Phys. Rev. A 1, 18 (1970).
- <sup>22</sup>D. Levesque, W.T. Ashurst, Phys. Rev. Lett. 33, 277 (1974).
- <sup>23</sup>M.H. Ernst, E.H. Hange and J.M.J. van Leeuwen, Phys. Rev. Lett. 25, 1254 (1970).

- <sup>24</sup>J.R. Dorfman, E.G.D. Cohen, Phys. Rev. Lett. 25, 1257 (1970).
- <sup>25</sup>Y. Pomeau, P. Resibois, Phys. Rep. C 19, 63 (1975).
- <sup>26</sup>J.R.D. Copley, S.W. Lovesey, Rep. Prog. Phys. 38, 461 (1975).
- <sup>27</sup>W. Schommers, Solid State Commun. 16, 45 (1975).
- <sup>28</sup>C. Hoheisel, Phys. Rev. A 23, 1998 (1981).
- <sup>29</sup>B.J. Berne, D. Forster, Ann. Rev. Chem. 22, 563 (1971).
- <sup>30</sup>R. Zwanzig, N.K. Ailawadi, Phys. Rev. 182, 280 (1969).
- <sup>31</sup>Y. Pomeau, Phys. Rev. A 7, 1134 (1973).
- <sup>32</sup>E. Schneider, private communication.
- <sup>33</sup>K. Kawasaki, Phys. Rev. 150, 291 (1966).
- <sup>34</sup>R. Block, Ges. Kernforschung, KfK 2488 (1977).
- <sup>35</sup>P.A. Egelstaff, "An Introduction to the Liquid State",  
(Academic, New York, 1967).
- <sup>36</sup>T. Gaskell, N.H. March, Phys. Lett. 33A, 460 (1970).